Synthesis and Structure of a Zirconium Dinitrogen Complex with a Side-On Bridging N_2 Unit

Jonathan D. Cohen,[†] Michael D. Fryzuk,*[,‡] Thomas M. Loehr,*[,†] Murugesapillai Mylvaganam,[‡] and Steven J. Rettig[‡,§]

Department of Chemistry, University of British Columbia, 2036 Main Mall, Vancouver, BC, Canada V6T 1Z1, and Department of Biochemistry and Molecular Biology, Oregon Graduate Institute of Science and Technology, Portland, Oregon 97291-1000

Received August 7, 1997[⊗]

Reduction of $Zr(O\text{-}2,6\text{-}Me_2C_6H_3)Cl_2[N(SiMe_2CH_2PPr^i_2)_2]$ with sodium amalgam under dinitrogen yields the dinuclear zirconium dinitrogen complex $\{[(Pr^i_2PCH_2SiMe_2)_2N]Zr(O\text{-}2,6\text{-}Me_2C_6H_3)\}_2(\mu\text{-}\eta^2\text{:}\eta^2\text{-}N_2)$. Solid state structural analysis shows that the dinitrogen unit is bound in a side-on mode of coordination with the N−N bond distance at 1.528(7) Å; resonance Raman spectra show a band at 751 cm^{-1} for ν(N−N), which is consistent with this very long bond. In addition, the N_2 ligand is hinged slightly so that the $Zr_2(\mu\text{-}\eta^2\text{:}\eta^2\text{-}N_2)$ core adopts a flattened butterfly shape rather than a completely planar core as found in other related systems. Other Zr(IV) precursors of the general formula $ZrCl_2X[N(SiMe_2CH_2PPr^i_2)_2]$ (X = OBu^t, $OCHPh_2$, NPh_2) either decompose upon reduction under N_2 or produce mixtures of products.

Introduction

"The fixation of dinitrogen is one of the great discoveries awaiting the ingenuity of chemists." These words[1] by William Crookes in 1898 foreshadowed the great discovery in 1905 of the Haber process,[2,3] which is presently used to produce millions of tons of ammonia from dinitrogen and dihydrogen. Nevertheless, for the coordination chemist, the challenge[4] still remains to activate N_2 under conditions milder than those typically used by BASF in the Haber−Bosch version[5] of this process. Although the coordination chemistry of the N_2 molecule has flourished under this challenge and much new fundamental knowledge has been gleaned,[6−12] no reaction comparable to the Haber discovery has yet been uncovered.

Recent fundamental studies on the binding of N_2 to metal complexes have shown some remarkable developments.[12] Not only do transition metals bind N_2 in a variety of bonding modes,[11] but complexation to lithium,[13] gold,[14] and samarium[15,16] has also been achieved. In addition, cleavage of dinitrogen by Mo(III) to form a molybdenum nitride species has been reported.[17,18] Recently, we described the preparation and structures of dinuclear complexes of zirconium that contain dinitrogen in either the side-on bridging or the end-on bridging mode of ligation.[19−21] Thus, $\{[(Pr^i_2PCH_2SiMe_2)_2N]ZrCl\}_2(\mu\text{-}\eta^2\text{:}\eta^2\text{-}N_2)$ (**1**) has the N_2 unit side-on with a N−N bond length of 1.548(7) Å, while $\{[(Pr^i_2PCH_2SiMe_2)_2N]Zr(\eta^5\text{-}Cp)\}_2(\mu\text{-}N_2)$ (**2**) has the dinitrogen ligand end-on with a N−N bond distance of 1.301(3) Å. By changing the ancillary ligand from a tridentate amidodiphosphine to a macrocyclic system containing two amido units, we were also able to prepare the side-on dinitrogen complex $\{[(PhP(CH_2SiMe_2NSiMe_2CH_2)_2PPh]Zr\}_2(\mu\text{-}\eta^2\text{:}\eta^2\text{-}N_2)$ (**3**); the N−N bond length is 1.43(4) Å, and the complex displays new modes of reactivity with H_2 and silanes.[19] We have also suggested[20] that the frontier orbitals of the zirconium center could be influenced by the ancillary ligands and matched to the π^* orbitals of the N_2 fragment in either the side-on or the end-on mode. Because of our continuing interest in fundamental studies of dinitrogen coordination, we embarked on a program to examine the effects of different ligand environments on the preparation and structure of zirconium dinitrogen complexes. In this paper, we summarize our efforts and provide another example of a side-on bound dinitrogen complex.

[†] Oregon Graduate Institute of Science and Technology.
[‡] University of British Columbia.
[§] Experimental Officer, UBC Structural Chemistry Laboratory.
[⊗] Abstract published in *Advance ACS Abstracts,* December 15, 1997.

(1) Crookes, W. *The Report of the 68th Meeting of the British Association for the Advancement of Science, Bristol*; John Murray: London, 1898.
(2) Feldman, M. R.; Tarver, M. L. *J. Chem. Educ.* **1983**, *60*, 463.
(3) Haber, F.; van Oordt, G. *Z. Anorg. Chem.* **1905**, *44*, 341.
(4) Green, M. L. H. *J. Chem. Soc., Dalton Trans.* **1991**, 575.
(5) Jennings, J. R. *Catalytic Ammonia Synthesis: Fundamentals and Practice*; Plenum Press: New York and London, 1991; Vol. 1.
(6) Sellmann, D. *Angew. Chem., Int. Ed. Engl.* **1974**, *13*, 639.
(7) Chatt, J.; Dilworth, J. R.; Richards, R. L. *Chem. Rev.* **1978**, *78*, 589.
(8) Henderson, R. A.; Leigh, G. J.; Pickett, C. J. *Adv. Inorg. Chem. Radiochem.* **1983**, *27*, 197.
(9) Pelikan, P.; Boca, R. *Coord. Chem. Rev.* **1984**, *55*, 55.
(10) Leigh, G. J. *Acc. Chem. Res.* **1992**, *25*, 177.
(11) Hidai, M.; Mizobe, Y. *Chem. Rev.* **1995**, *95*, 1115.
(12) Gambarotta, S. *J. Organomet. Chem.* **1995**, *500*, 117.
(13) Ho, J.; Drake, R. J.; Stephan, D. W. *J. Am. Chem. Soc.* **1993**, *115*, 3792.
(14) Sharp, P. R.; Shan, H.; Yan, Y.; James, A. J. *Science* **1997**, *275*, 1460.
(15) Evans, W. J.; Ulibarri, T. A.; Ziller, J. W. *J. Am. Chem. Soc.* **1988**, *110*, 6877.
(16) Jubb, J.; Gambarotta, S. *J. Am. Chem. Soc.* **1994**, *116*, 4477.
(17) Laplaza, C. E.; Cummins, C. C. *Science* **1995**, *268*, 861.
(18) Laplaza, C. E.; Johnson, M. J. A.; Peters, J. C.; Odom, A. L.; Kim, E.; Cummins, C. C.; George, G. N.; Pickering, I. J. *J. Am. Chem. Soc.* **1996**, *118*, 8623.
(19) Fryzuk, M. D.; Love, J. B.; Rettig, S. J.; Young, V. G. *Science* **1997**, *275*, 1445.
(20) Fryzuk, M. D.; Haddad, T. S.; Mylvaganam, M.; McConville, D. H.; Rettig, S. J. *J. Am. Chem. Soc.* **1993**, *115*, 2782.
(21) Cohen, J. D.; Mylvaganam, M.; Fryzuk, M. D.; Loehr, T. M. *J. Am. Chem. Soc.* **1994**, *116*, 9529.

S0020-1669(97)00978-6 CCC: $15.00
Published on Web 01/12/1998

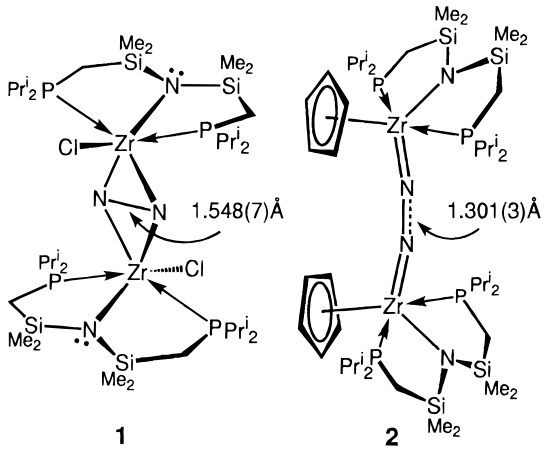

1 **2**

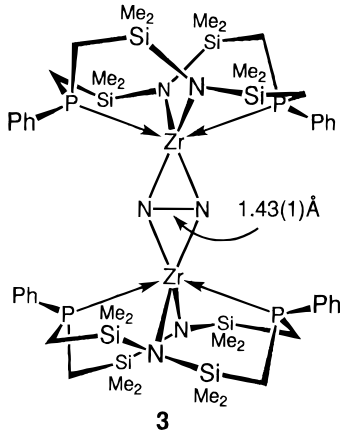

3

Experimental Section

General Procedures. All manipulations were performed under prepurified nitrogen in a Vacuum Atmospheres HE-553-2 work station equipped with an MO-40-2H purification system or in Schlenk-type glassware. Pentane, diethyl ether, and hexanes were dried and deoxygenated by distillation from sodium−benzophenone ketyl under argon. Toluene was predried by refluxing over CaH_2 and then distilled from sodium under argon. Tetrahydrofuran and hexanes were predried by refluxing over CaH_2 and then distilled from sodium−benzophenone ketyl under argon. Deuterated benzene (C_6D_6, 99.6 atom % D) and deuterated toluene (C_7D_8, 99.6 atom % D), purchased from MSD Isotopes, were dried over activated 4-Å molecular sieves, vacuum-transferred, and freeze-pump-thawed three times before use.

Dinitrogen gas was purified by purging through a column containing MnO and activated 4-Å molecular sieves. The 99% $^{15}N_2$ was obtained from Cambridge Isotopes Ltd. and was used as supplied.

The ^1H, ^{31}P, and ^{13}C NMR spectra were recorded on a Varian XL-300, a Bruker AC 200, a Bruker WH-400, or a Bruker AM 500 spectrometer. Proton spectra were referenced using the partially deuterated solvent peak as the internal reference, C_6D_5H at 7.15 ppm and $C_6D_5CD_2H$ at 2.09 ppm relative to Me_4Si. The $^{31}P\{^1H\}$ NMR spectra were referenced to external $P(OMe)_3$ set at +141.00 ppm relative to 85% H_3PO_4. The $^{13}C\{^1H\}$ NMR spectra were referenced to the C_6D_6 signal at 128.0 ppm or to the $CD_3C_6D_5$ signal at 20.4 ppm. Solution $^{15}N\{^1H\}$ NMR spectra were recorded on the Varian XL-300, referenced to external formamide set at 0.00 ppm. Solid-state ^{15}N NMR spectra were run on a Bruker MSL-400, referenced to solid NH_4Cl set at −73.39 ppm with respect to neat formamide at 0.00 ppm. $^1H\{^{31}P\}$ NMR spectra were recorded on the Bruker AM 500 spectrometer.

Resonance Raman spectra[21] were recorded on a modified Jarrell-Ash model 25-300 Raman spectrometer. Excitation radiation was supplied by Spectra Physics Ar^+ and Kr^+ lasers operating at 514.5 and 647.1 nm, respectively. Raman light was collected in a backscattering geometry. Multiple scans were collected and calibrated against indene, toluene, or THF as external standards for peak positions. All wavenumber assignments were estimated to be accurate within 2 cm^{-1}. Spectra for polarization studies of solution samples were collected in a 90° scattering geometry at 278 K on a Dilor Z-24 Raman spectrophotometer. Typical slit-width settings were between 5 and 9 cm^{-1}. All samples were sealed under N_2 in 1.5−1.8 × 90 mm Kimax glass capillary tubes.

UV−vis spectra were recorded on a Perkin Elmer 5523 UV/Vis spectrophotometer stabilized at 20 °C. Mass spectral studies were carried out on a Kratos MS 50 using an EI source. IR spectra were recorded on a Bomem MB-100 spectrometer. Solution samples were recorded in a 0.1 mm KBr cell, and solid samples were recorded as KBr pellets. Carbon, hydrogen, and nitrogen analyses were performed by the microanalyst of the UBC Chemistry Department.

The starting complex $ZrCl_3[N(SiMe_2CH_2PPr^i_2)_2]$ was prepared according to the published procedure.[22] Mercury was purchased from BDH and purified as follows: In a separatory funnel, mercury (500 g) was washed with 2 M HCl (2 × 25 mL) acid and then with distilled water (2 × 50 mL), and it was finally rinsed a few times with Et_2O (25 mL) until no further gray color was present in the ether washings. During washings, a slag was formed on the surface of the Hg which was separated from the shiny Hg. Pure Hg was dried under vacuum for 12 h. Sodium amalgam was made under a nitrogen atmosphere and washed with toluene (2 × 25 mL) until the washings showed no gray coloration.

The sodium alkoxide and aryloxide reagents, $NaOCHPh_2$ and NaO-2,6-$Me_2C_6H_3$, were prepared by reacting a toluene solution of the alcohol with sodium (3 h at room temperature (RT) followed by a 3 h reflux). The resulting white solid was filtered off and extracted with THF (to remove finely dispersed sodium), and the THF was removed under vacuum to give alcohol-free NaOR. Prior to the reaction, the alcohol was dissolved in toluene, and the solution was stirred with Mg turnings (0.1 equiv) for 12 h, and the mixture was filtered. $KOBu^t$ was purchased from Aldrich and was sublimed prior to use. The sodium amide, $NaNPh_2$, was prepared by reacting the amine, $HNPh_2$, with NaN-$(SiMe_3)_2$ in toluene. The $NaNPh_2$ was precipitated out of toluene, collected on a frit, and washed with hexanes to obtain pure material.

Zr(O-2,6-$Me_2C_6H_3$)Cl_2[N($SiMe_2CH_2PPr^i_2$)$_2$], 5. To a solution of $ZrCl_3[N(SiMe_2CH_2PPr^i_2)_2]$, **4** (4.00 g, 5.08 mmol), in toluene (150 mL) was added solid Na(O-2,6-$Me_2C_6H_3$) (1.03 g, 6.35 mmol) in three portions at 1 h intervals at RT. The reaction mixture was stirred for 16 h, and then the salt (NaCl) was removed by filtering through Celite. The filtrate was concentrated to 25 mL, an equal volume of hexanes added, and the mixture allowed to stand at room temperature for 24 h. A colorless crystalline product slowly separated from the solution (2.41 g, 70%). ^1H NMR (δ, 300 MHz, C_6D_6): 0.48 (s, 12H, Si(CH_3)$_2$); 0.96 (d of d, 16H, 12H of P[CH(CH_3)$_2$]$_2$ and 4H of SiCH_2P, $^3J_{H-H}$ = 6.1 Hz, $^3J_{P-H}$ = 14.0 Hz); 1.06 (d of d, 12H, P[CH(CH_3)$_2$]$_2$, $^3J_{H-H}$ = 6.1 Hz, $^3J_{P-H}$ = 14.0 Hz); 2.00 (sept of t, 4H, P[CH(CH_3)$_2$]$_2$, $^3J_{H-H}$ = 6.1 Hz, $^2J_{P-H}$ = 2.0 Hz); 2.80 (s, 6H, 2, 6-Me_2Ph); 6.82 (t, 1H, *p*-Ph, $^3J_{H-H}$ = 7.4 Hz); 7.05 (d, 2H, *m*-Ph, $^3J_{H-H}$ = 7.4 Hz). $^{31}P\{^1H\}$ NMR (δ, 121.421 MHz, C_6D_6): 14.98 (s). $^{13}C\{^1H\}$ NMR (δ, 50.323 MHz, C_6D_6): 5.41 (s, Si(CH_3)$_2$); 10.70 (s, SiCH_2P); 19.07 (s, P[CH(CH_3)$_2$]$_2$); 19.15 (s, P[CH(CH_3)$_2$]$_2$); 19.86 (s, 2,6-Me_2Ph); 24.09 (t, P[CH(CH_3)$_2$]$_2$, $^2J_{C-P}$ = 6.2 Hz); 120.94 (s, *p*-Ph); 128.79 (s, *m*-Ph). Anal. Calcd for $C_{26}H_{53}Cl_2NOP_2Si_2Zr$: C, 46.20; H, 7.90; N, 2.07. Found: C, 46.07; H, 8.10; N, 2.03.

Zr(OBu^t)Cl_2[N($SiMe_2CH_2PPr^i_2$)$_2$], 6. To a solution of $ZrCl_3$-$[N(SiMe_2CH_2PPr^i_2)_2]$ (1.50 g, 2.54 mmol) in Et_2O (60 mL) was added a solution of $KOBu^t$ (285 mg, 2.54 mmol) in Et_2O (10 mL) at RT, and the mixture was stirred for 3 h. The solvent was stripped off under vacuum the residues were extracted with pentane (40 mL), and the extracts were filtered through a layer of Celite. Stripping off the solvent gave a colorless oil containing >80% (by ^1H NMR spectroscopy) of the desired product. ^1H NMR (δ, 300 MHz, C_6D_6): 0.45 (s, 12H, Si-(CH_3)$_2$); 1.05 (d, 4H, SiCH_2P, $^2J_{P-H}$ = 5.7 Hz); 1.32 and 1.35 (each d of d, 24H, P[CH(CH_3)$_2$]$_2$, $^3J_{P-H}$ = 2.9 Hz, $^3J_{H-H}$ = 7.6 Hz); 1.50 (s, 9H, OC(CH_3)$_3$); 2.04 (t of sept, 4H, P[CH(CH_3)$_2$]$_2$, $^2J_{P-H}$ = 1.9 Hz, $^3J_{H-H}$ = 7.6 Hz). $^{31}P\{^1H\}$ NMR (δ, 81.015 MHz, C_6D_6): 11.60 (s).

(22) Fryzuk, M. D.; Carter, A.; Westerhaus, A. *Inorg. Chem.* **1985**, *24*, 642.

Table 1. $^1H\{^{31}P\}$ NMR Data for Complexes **9** and **9a**

groups	major isomer (δ)	minor isomer (δ)
$Si(CH_3)_2$	0.37 (s, 12H)	0.29 (s, 6H), 0.32 (s. 6H)
	0.41 (s, 12H)	0.32 (s, 6H), 0.35 (s, 6H)
$SiCH_2P$	1.30 (d, 4H, $^2J_{H-H} = 1.6$ Hz)	obscured
	1.32 (d, 4H, $^2J_{H-H} = 1.6$ Hz)	
$P[CH(CH_3)_2]_2$	1.04 (d, 12H, $^3J_{H-H} = 6.7$ Hz)	1.13 (d, 6H), 1.26 (d, 6H)
	1.05 (d, 12H, $^3J_{H-H} = 6.7$ Hz)	1.34 (d, 6H), 1.44 (d, 6H)
	1.17 (d, 12H, $^3J_{H-H} = 7.3$ Hz)	rest of the resonances were obscured
	1.23 (d, 12H, $^3J_{H-H} = 7.3$ Hz)	
$P[CH(CH_3)_2]_2$	2.03 (sept, 4H, $^3J_{H-H} = 7.3$ Hz)	2.04 (sept, 2H, $^3J_{H-H} = 7.4$ Hz)
	2.39 (sept, 4H, $^3J_{H-H} = 6.7$ Hz)	2.20 (sept, 2H, $^3J_{H-H} = 7.4$ Hz)
		2.48 (sept, 2H, $^3J_{H-H} = 7.4$ Hz)
		2.53 (sept, 2H, $^3J_{H-H} = 7.4$ Hz)
2,6-Me_2Ph	2.34 (s, 12H)	only assignable resonance was a broad peak at 2.32
p-Ph	6.66 (t, 2H, $^3J_{H-H} = 7.1$ Hz)	6.62 (t, 2H, $^3J_{H-H} = 6.9$ Hz)
m-Ph	7.00 (t, 4H, $^3J_{H-H} = 7.1$ Hz)	6.98 (t, 4H, $^3J_{H-H} = 6.9$ Hz)

$Zr(OCHPh_2)Cl_2[N(SiMe_2CH_2PPr^i_2)_2]$, 7. The complex was prepared by a procedure similar to the one described above for **6**, using $ZrCl_3[N(SiMe_2CH_2PPr^i_2)_2]$ (1.25 g, 2.12 mmol) and $Ph_2CHONa\cdot THF$ (589 mg, 2.12 mmol). The product was crystallized from a solvent mixture containing Et_2O and pentane (1.23 g, 78%). ^1H NMR (δ, 200.132 MHz, C_6D_6): 0.50 (s, 12H, $Si(CH_3)_2$); 0.94 (m, 28H, $SiCH_2P$ and $P[CH(CH_3)_2]_2$); 1.73 (sept, 4H, $P[CH(CH_3)_2]_2$, $^3J_{H-H} = 6.8$ Hz); 6.82 (s, 1H, *CH*Ph); 7.00 (2H, t, *p*-Ph, $^3J_{H-H} = 7.6$ Hz); 7.16 (4H, t, *m*-Ph, $^3J_{H-H} = 7.6$ Hz); 7.71 (4H, d, *o*-Ph, $^3J_{H-H} = 7.6$ Hz). $^{31}P\{^1H\}$ NMR (δ, 81.015 MHz, C_6D_6): 13.53 (s). Anal. Calcd for $C_{31}H_{55}Cl_2ONP_2Si_2Zr$: C, 50.45; H, 7.51; N, 1.90. Found: C, 51.25; H, 7.67; N, 1.76.

$Zr(NPh_2)Cl_2[N(SiMe_2CH_2PPr^i_2)_2]$, 8. To a solution of $ZrCl_3[N(SiMe_2CH_2PPr^i_2)_2]$ (1.25 g, 2.12 mmol) in THF (60 mL) was added a solution of $NaNPh_2$ (199 mg, 2.12 mmol) in THF (20 mL) at RT, and the mixture was stirred for 2 h. The solvent was stripped off under vacuum, the residues were extracted with toluene (20 mL), and the extracts were filtered through a layer of Celite. The product was crystallized from a solvent mixture containing toluene and hexanes (1.15 g, 75%). ^1H NMR (δ, 400 MHz, C_6D_6): 0.47 (s, 12H, $Si(CH_3)_2$); 1.16 and 1.10 (m, 28H, $SiCH_2P$ and $P[CH(CH_3)_2]_2$); 2.12 (sept, 4H, $P[CH(CH_3)_2]_2$, $^3J_{H-H} = 4.0$ Hz); 6.96 (2H, t, *p*-Ph, $^3J_{H-H} = 8.0$ Hz); 7.23 (4H, t, *m*-Ph, $^3J_{H-H} = 8.0$ Hz); 7.30 (4H, d, *o*-Ph, $^3J_{H-H} = 8.0$ Hz). $^{31}P\{^1H\}$ NMR (δ, 81.015 MHz, C_6D_6): 15.58 (s). $^{31}P\{^1H\}$ NMR in a solvent mixture containing THF and C_6D_6 (δ): 2.70 (br); −1.20 (br). $^{13}C\{^1H\}$ NMR (δ, 50.323 MHz, C_6D_6): 5.04 (s, $SiCMe_2$); 9.69 (s, CH_2Si); 18.85 and 19.59 (s, $CH(CH_3)_2$); 24.28 (t, $CH(CH_3)_2$, $^1J_{P-C} = 5.6$ Hz); 123.41 (s, Ph); 126.98 (s, Ph); 128.26 (s, Ph). Anal. Calcd for $C_{30}H_{54}Cl_2N_2P_2Si_2Zr$: C, 49.83; H, 7.53; N, 3.88. Found: C, 50.09; H, 7.56; N, 4.00.

$\{[(Pr^i_2PCH_2SiMe_2)_2N]Zr(O\text{-}2,6\text{-}Me_2C_6H_3)\}_2(\mu\text{-}\eta^2\text{:}\eta^2\text{-}N_2)$, 9. A solution of $Zr(O\text{-}2,6\text{-}Me_2\text{-}C_6H_3)Cl_2[N(SiMe_2CH_2PPr^i_2)_2]$ (1.05 g, 1.48 mmol) in toluene (100 mL) was transferred into a thick-walled reaction flask (300 mL) containing Na/Hg (80 g of 0.17% amalgam, 5.74 mmol of Na). The flask was then cooled to −196 °C, filled with 1 atm of N_2, sealed, and allowed to warm slowly to RT with stirring. The colorless solution slowly took on the deep blue color of the product. The reaction mixture was stirred for 5 d; the solution was then decanted from the amalgam and filtered through a layer of Celite. The amalgam-containing residue was extracted with several 50 mL portions (approximately 400 mL) of toluene, until the extracts showed no blue color. The filtrate and the extracts were combined, and stripping off the solvent gave a deep blue solid, which was washed with hexanes (2 × 25 mL). Pure product was obtained by slow evaporation of a toluene solution of the crude product at RT (0.36 g, 40%). $^1H\{^{31}P\}$ NMR (δ, 500 MHz, C_7D_8): see Table 1. $^{31}P\{^1H\}$ NMR (δ, 121.421 MHz, C_7D_8), at 20 °C: major isomer 8.69 (s); minor isomer 8.85 (s) and 11.26 (s). NOEDIFF experiments (δ, 400 MHz, C_7D_8): irradiating the resonances at 7.00 or 6.98 ppm showed enhancements at 2.34 and 2.32 ppm. Variable-temperature $^{31}P\{^1H\}$ NMR (δ, 121.42 MHz, C_7D_8): upon cooling of a sample of pure major isomer, the resonance at 8.69 ppm broadened and below −40 °C began to show shoulders at 7.60 and 9.10 ppm. Below −78 °C, a broad peak began to appear at 4.00 ppm and increased in intensity with decreasing temperature (down to −93 °C). Anal. Calcd for a sample containing only the major isomer, $C_{26}H_{53}ON_2P_2Si_2Zr$: C, 50.44; H, 8.63; N, 4.53. Found: C, 50.70; H, 8.87; N, 4.33. Anal. Calcd for a sample containing a mixture of major isomer and minor isomer (major:minor = 2:1), $C_{26}H_{53}ON_2P_2Si_2Zr$: C, 50.44; H, 8.63; N, 4.53. Found: C, 50.24; H, 8.71; N, 4.29. Resonance Raman (cm^{-1}), solid ($^{14}N_2$): 258m, 314vs, 350w, 595m, 732s, 751s, 989w, 1046m. MS (EI), *m/z*: 1236, 1193, 1107, 1063, 1007, 975, 695, 350, 262.

$\{[(Pr^i_2PCH_2SiMe_2)_2N]Zr(O\text{-}2,6\text{-}Me_2C_6H_3\}_2(\mu\text{-}\eta^2\text{:}\eta^2\text{-}^{15}N_2)$, 9-$^{15}N_2$. The nitrogen-15 analogue was prepared by a procedure similar to that for **9**, but by introducing $^{15}N_2$ gas into the flask containing the degassed reaction mixture. Workup was carried out under unlabeled N_2. $^{15}N\{^1H\}$ NMR (δ, 30.406 MHz, C_7D_8): minor isomer, **9a**, 342.91 (s); major isomer, **9**, 339.06 (s). Resonance Raman (cm^{-1}), solid ($^{15}N_2$): 277m, 309s, 350w, 576m, 596w, 725s, 750w, 1006vw, 1031w. MS (EI), *m/z*: 1238, 1195, 1111, 977, 696, 350, 262.

$\{[(Pr^i_2PCH_2SiMe_2)_2N]Zr(OBu^t)\}_2(\mu\text{-}\eta^2\text{:}\eta^2\text{-}N_2)$, 10. A solution of crude $Zr(OBu^t)Cl_2[N(SiMe_2CH_2PPr^i_2)_2]$ (approximately 1.05 g, 1.48 mmol) was dissolved in toluene (100 mL), and the solution was transferred into a thick-walled reaction flask (300 mL) containing Na/Hg (80 g of 0.30% amalgam, 10.4 mmol of Na). The flask was then cooled to −196 °C, filled with 1 atm of N_2, sealed, and allowed to warm slowly to RT with stirring. The colorless solution slowly took on the deep purple color of the product. The reaction mixture was stirred for 5 d, and the solution was decanted and filtered through a layer of Celite. Stripping off the solvent from the filtrate gave a dark purple oil. Attempts to crystallize the product were not successful. ^1H NMR (δ, 300 MHz, C_6D_6): 0.46 and 0.42 (s, 12H, $Si(CH_3)_2$); 1.24 (br m, 28H, $SiCH_2P$ and $P[CH(CH_3)_2]_2$); 1.42 (s, 9H, $OC(CH_3)_3$); 1.97 (br sept, 2H, $P[CH(CH_3)_2]_2$, $^3J_{H-H} = 7.2$ Hz); 2.25 (br sept, 2H, $P[CH(CH_3)_2]_2$, $^3J_{H-H} = 6.6$ Hz). $^{31}P\{^1H\}$ NMR (δ, 81.015 MHz, C_6D_6): 8.16 (s). $^{15}N\{^1H\}$ NMR (δ, 30.406 MHz, C_7D_8): 346.41 (s); 334.35 (s); 319.64 (s); 254.87 (s); 248.86 (s).

X-ray Crystallographic Analyses of $Zr(O\text{-}2,6\text{-}Me_2C_6H_3)Cl_2[N(SiMe_2CH_2PPr^i_2)_2]$, 5, and $\{[(Pr^i_2PCH_2SiMe_2)_2N]Zr(O\text{-}2,6\text{-}Me_2C_6H_3)\}_2(\mu\text{-}\eta^2\text{:}\eta^2\text{-}N_2)$, 9. Crystallographic data appear in Table 2. The final unit-cell parameters were obtained by least-squares calculations on the setting angles for 25 reflections with $2\theta = 29.6-36.1°$ for **5** and 46.4−72.7° for **9**. The intensities of three standard reflections, measured every 200 reflections throughout the data collections, decayed linearly for both **5** (1.3%) and **9** (2.0%). The data were processed[23] and corrected for Lorentz and polarization effects, decay, and absorption (empirical; based on azimuthal scans).

The structures were solved by the Patterson method. The dinuclear molecule **9** lies on a center of symmetry in the unit cell. The non-hydrogen atoms were refined with anisotropic thermal parameters. Hydrogen atoms were fixed in calculated positions with C−H = 0.98 Å and $B_H = 1.2B_{\text{bonded atom}}$. Secondary extinction corrections were applied (Zachariasen type 1 isotropic), the final values of the extinction

(23) *Crystal Structure Analysis Package*; Version 1.7; Molecular Structure Corp.: The Woodlands, TX, 1995.

Table 2. Crystallographic Data

	5	**9**
formula	$C_{26}H_{53}Cl_2NOP_2Si_2Zr$	$C_{52}H_{106}N_4O_2P_4Si_4Zr_2$
fw	675.96	1238.11
crystal system	monoclinic	orthorhombic
space group	$P2_1/c$ (No. 14)	*Pbcn* (No. 60)
a, Å	13.442(2)	14.3839(14)
b, Å	16.777(2)	17.7539(14)
c, Å	16.456(2)	25.9967(10)
β, deg	108.564(9)	90
V, Å^3	3518.1(7)	6638.8(7)
Z	4	4
ρ_{calcd}, g/cm^3	1.276	1.239
T, °C	21	21
radiation	Mo	Cu
λ, Å	0.710 69	1.541 78
μ, cm^{-1}	0.64	4.55
R^a	0.035	0.037
$R_w{}^b$	0.031	0.034

^{a} $R = \sum||F_o| - |F_c||/\sum|F_o|$. ^{b} $R_w = [\sum w(|F_o| - |F_c|)^2/\sum w|F_o|^2]^{1/2}$.

Table 3. Selected Bond Lengths (Å) and Angles (deg) for $Zr(O\text{-}2,6\text{-}Me_2C_6H_3)Cl_2[N(SiMe_2CH_2PPr^i{}_2)_2]$, **5**

Zr(1)−Cl(1)	2.4732(9)	Zr(1)−Cl(2)	2.4450(9)
Zr(1)−P(1)	2.790(1)	Zr(1)−P(2)	2.769(1)
Zr(1)−O(1)	1.969(2)	Zr(1)−N(1)	2.166(2)
P(1)−C(1)	1.819(4)	P(1)−C(7)	1.844(3)
P(1)−C(8)	1.848(3)	P(2)−C(2)	1.821(3)
P(2)−C(13)	1.842(3)	P(2)−C(14)	1.846(3)
Si(1)−N(1)	1.733(3)	Si(1)−C(1)	1.892(4)
Si(1)−C(3)	1.880(4)	Si(1)−C(4)	1.863(4)
Si(2)−N(1)	1.736(3)	Si(2)−C(2)	1.894(3)
Si(2)−C(5)	1.879(4)	Si(2)−C(6)	1.862(4)
O(1)−C(19)	1.362(4)		

Cl(1)−Zr(1)−Cl(2)	177.14(3)	Cl(1)−Zr(1)−P(1)	91.25(3)
Cl(1)−Zr(1)−P(2)	79.16(3)	Cl(1)−Zr(1)−O(1)	90.07(7)
Cl(1)−Zr(1)−N(1)	92.03(7)	Cl(2)−Zr(1)−P(1)	91.34(3)
Cl(2)−Zr(1)−P(2)	98.91(3)	Cl(2)−Zr(1)−O(1)	88.34(7)
Cl(2)−Zr(1)−N(1)	89.75(7)	P(1)−Zr(1)−P(2)	155.58(3)
P(1)−Zr(1)−O(1)	98.77(6)	P(1)−Zr(1)−N(1)	76.57(7)
P(2)−Zr(1)−O(1)	103.60(6)	P(2)−Zr(1)−N(1)	81.34(7)
O(1)−Zr(1)−N(1)	174.92(9)	Zr(1)−P(1)−C(1)	97.5(1)
Zr(1)−P(1)−C(7)	125.0(1)	Zr(1)−P(1)−C(8)	110.2(1)
C(1)−P(1)−C(7)	107.4(2)	C(1)−P(1)−C(8)	107.0(2)
C(7)−P(1)−C(8)	108.1(2)	Zr(1)−P(2)−C(2)	99.5(1)
Zr(1)−P(2)−C(13)	115.1(1)	Zr(1)−P(2)−C(14)	122.9(1)
C(2)−P(2)−C(13)	104.1(2)	C(2)−P(2)−C(14)	105.4(2)
C(13)−P(2)−C(14)	107.3(2)	N(1)−Si(1)−C(1)	107.8(1)
N(1)−Si(1)−C(3)	113.8(2)	N(1)−Si(1)−C(4)	114.2(1)
C(1)−Si(1)−C(3)	106.6(2)	C(1)−Si(1)−C(4)	107.2(2)
C(3)−Si(1)−C(4)	106.7(2)	N(1)−Si(2)−C(2)	109.4(1)
N(1)−Si(2)−C(5)	113.3(1)	N(1)−Si(2)−C(6)	112.6(1)
C(2)−Si(2)−C(5)	107.6(2)	C(2)−Si(2)−C(6)	106.5(2)
C(5)−Si(2)−C(6)	107.1(2)	Zr(1)−O(1)−C(19)	170.5(2)
Zr(1)−N(1)−Si(1)	120.9(1)	Zr(1)−N(1)−Si(2)	121.2(1)
Si(1)−N(1)−Si(2)	117.9(1)		

coefficients being 2.05(5) × 10^{-7} for **5** and 9.2(5) × 10^{-8} for **9**. Neutral-atom scattering factors and anomalous dispersion corrections were taken from ref 24.

Selected bond lengths and bond angles for the **5** and **9** appear in Tables 3 and 4, respectively. Tables of final atomic coordinates and equivalent isotropic thermal parameters, anisotropic thermal parameters, bond lengths and angles, torsion angles, intermolecular contacts, and least-squares planes are included as Supporting Information.

Results and Discussion

Synthesis and Structure of Zr(IV) Precursors. Each end of the side-on dinitrogen complex **1** contains a $ZrCl[N(SiMe_2CH_2PPr^i{}_2)_2]$ fragment. We reasoned that replacement of the chloride by another hard, anionic ligand, such as an alkoxide (OR) or an amide (NR_2), should not drastically affect the frontier orbitals of the fragment, and thus, a dinitrogen complex with the N_2 side-on bound should result. This premise was based on semiempirical calculations on the fragments *trans*-$Zr(NH_2)X(PH_3)_2$, which show that, for X = halide, OH, or NH_2, the two metal-based orbitals that are available to overlap with the π^* orbitals on the N_2 fragment are those that prefer the side-on mode.[20] Our initial attempts to utilize the dinitrogen complex **1** as the starting material by direct substitution of the Cl ligand failed since addition of a variety of alkoxide or aryloxide reagents to **1** resulted in either decomposition or no reaction. However, as the starting material for both **1** and **2** is the Zr(IV) complex $ZrCl_3[N(SiMe_2CH_2PPr^i{}_2)_2]$ (**4**), we examined functionalization of this complex.

Addition of 1 equiv of sodium 2,6-dimethylphenolate or potassium *tert*-butoxide to **4** resulted in the conversion to the derivatives $Zr(OR)Cl_2[N(SiMe_2CH_2PPr^i{}_2)_2]$ (**5**, R = 2,6-$Me_2C_6H_3$; **6**, R = Bu^t); sodium diphenylmethoxide, $NaOCHPh_2$, also produced the monoalkoxo complex **7**. In the case of the *tert*-butoxide complex **6**, we were unable to purify it from a number of side products, and this complicated reduction under N_2. However, we were able to prepare both the aryloxide derivative **5** and the substituted alkoxide **7** in high purity. In addition, the diphenylamido complex $Zr(NPh_2)Cl_2[N(SiMe_2CH_2PPr^i{}_2)_2]$ (**8**) was synthesized by a similar metathesis process using sodium diphenylamide.

The stereochemistry of these monosubstituted complexes is assumed to be distorted octahedral with the alkoxide, aryloxide, or amide trans to the amide of the ancillary tridentate ligand.

Table 4. Selected Bond Lengths (Å) and Angles (deg) for $\{[(Pr^i{}_2PCH_2SiMe_2)_2N]Zr(O\text{-}2,6\text{-}Me_2C_6H_3)\}_2(\mu\text{-}\eta^2\text{:}\eta^2\text{-}N_2)$, **9**^{a}

Zr(1)−P(1)	2.818(1)	Zr(1)−P(2)	2.846(1)
Zr(1)−O(1)	2.020(3)	Zr(1)−N(1)	2.211(3)
Zr(1)−N(2)	2.034(4)	Zr(1)−N(2)′	2.082(4)
P(1)−C(1)	1.824(5)	P(1)−C(7)	1.848(6)
P(1)−C(8)	1.851(6)	P(2)−C(2)	1.813(5)
P(2)−C(13)	1.844(5)	P(2)−C(14)	1.852(6)
Si(1)−N(1)	1.718(4)	Si(1)−C(1)	1.890(5)
Si(1)−C(3)	1.878(6)	Si(1)−C(4)	1.870(6)
Si(2)−N(1)	1.720(4)	Si(2)−C(2)	1.887(5)
Si(2)−C(5)	1.861(6)	Si(2)−C(6)	1.881(5)
O(1)−C(19)	1.331(6)	N(2)−N(2)′	1.528(7)

P(1)−Zr(1)−P(2)	145.54(4)	P(1)−Zr(1)−O(1)	87.6(1)
P(1)−Zr(1)−N(1)	79.4(1)	P(1)−Zr(1)−N(2)	128.10(10)
P(1)−Zr(1)−N(2)′	85.10(10)	P(2)−Zr(1)−O(1)	88.1(1)
P(2)−Zr(1)−N(1)	74.5(1)	P(2)−Zr(1)−N(2)	82.89(10)
P(2)−Zr(1)−N(2)′	126.19(10)	O(1)−Zr(1)−N(1)	123.0(1)
O(1)−Zr(1)−N(2)	119.8(1)	O(1)−Zr(1)−N(2)′	119.1(1)
N(1)−Zr(1)−N(2)	111.4(1)	N(1)−Zr(1)−N(2)′	114.7(1)
N(2)−Zr(1)−N(2)′	43.6(2)	Zr(1)−P(1)−C(1)	101.3(2)
Zr(1)−P(1)−C(7)	115.1(2)	Zr(1)−P(1)−C(8)	120.1(2)
C(1)−P(1)−C(7)	106.3(3)	C(1)−P(1)−C(8)	104.9(3)
C(7)−P(1)−C(8)	107.6(3)	Zr(1)−P(2)−C(2)	93.3(2)
Zr(1)−P(2)−C(13)	115.8(2)	Zr(1)−P(2)−C(14)	124.4(2)
C(2)−P(2)−C(13)	102.3(2)	C(2)−P(2)−C(14)	106.5(3)
C(13)−P(2)−C(14)	109.9(3)	N(1)−Si(1)−C(1)	110.3(2)
N(1)−Si(1)−C(3)	115.4(2)	N(1)−Si(1)−C(4)	112.3(2)
C(1)−Si(1)−C(3)	107.7(3)	C(1)−Si(1)−C(4)	105.4(2)
C(3)−Si(1)−C(4)	105.1(3)	N(1)−Si(2)−C(2)	108.2(2)
N(1)−Si(2)−C(5)	112.4(2)	N(1)−Si(2)−C(6)	115.4(2)
C(2)−Si(2)−C(5)	107.7(2)	C(2)−Si(2)−C(6)	106.3(2)
C(5)−Si(2)−C(6)	106.4(3)	Zr(1)−O(1)−C(19)	161.5(4)
Zr(1)−N(1)−Si(1)	123.9(2)	Zr(1)−N(1)−Si(2)	116.4(2)
Si(1)−N(1)−Si(2)	119.7(2)	Zr(1)−N(2)−Zr(1)′	130.7(2)
Zr(1)−N(2)−N(2)′	69.9(2)	Zr(1)′−N(2)−N(2)′	66.5(2)

^{a} Primes refer to the symmetry operation: $-x, y, {}^1/_2 - z$.

(24) (a) *International Tables for X-Ray Crystallography*; Kynoch Press: Birmingham, U.K., 1974; Vol. IV, pp 99−102. (b) *International Tables for Crystallography*; Kluwer Academic Publishers: Boston, MA, 1992; Vol. C, pp 200−206.

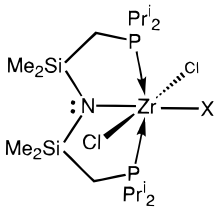

4 X = Cl
5 X = O-2,6-$Me_2C_6H_3$
6 X = OBu^t
7 X = $OCHPh_2$
8 X = NPh_2

All of the complexes **5**−**8** show very similar NMR spectral characteristics consistent with C_{2v} molecular symmetry; in particular, the silylmethyl protons ($SiMe_2$) appear as a singlet in the ^{1}H NMR spectrum and the methylene protons of the backbone (PCH_2Si) give rise to a simple doublet due to coupling to phosphorus-31. This stereochemistry was confirmed for the aryloxide complex **5** in the solid state.

The molecular structure and numbering scheme are shown in Figure 1, and selected bond lengths and angles are given in Table 3. The distortion away from octahedral is most evident in the P(1)−Zr(1)−P(2) angle of 155.58(3)° whereas the other transoid angles are closer to 180°: O(1)−Zr(1)−N(1) is 174.92(9)° and Cl(1)−Zr−Cl(2) is 177.14(3)°. In addition, the Zr(1)−O(1)−C(19) bond angle of 170.5(2)° indicates that there is some multiple-bond character in the Zr−O bond possibly due to π-donation from the oxygen to Zr. The Zr(1)−O(1) bond length of 1.969(2) Å is short as compared to those of other systems.[25] These two interrelated structural features are indicators of metal−oxygen $d_\pi-p_\pi$ interactions where larger bond angles and shorter bond lengths are correlated with π-electron donation from the oxygen.[25] By comparison, parameters associated with the zirconium−oxygen bond for $\{[(Bu^t)_3CO]_2ZrCl_3\cdot Li(OEt_2)_2\}$[25] are 1.859 Å and 169°; for $[Cp_2Zr(NMe_2)(O\text{-}2,6\text{-}Bu^t{}_2C_6H_3)]$,[26] they are 2.056(1) Å and 142.7(7),° and for $[(Cp_2ZrMe)_2O]$,[27] 1.945 Å and 174.1° are found. Other bond lengths are typical of those previously found for Zr(IV) complexes with this particular ligand system.[20]

Reduction under Dinitrogen. The reaction of aryloxide **5** with >2 equiv of Na/Hg in toluene under 1−4 atm of N_2 produced the dinuclear dinitrogen complex $\{[(Pr^i{}_2PCH_2SiMe_2)_2N]Zr(O\text{-}2,6\text{-}Me_2C_6H_3)\}_2(\mu\text{-}\eta^2\text{:}\eta^2\text{-}N_2)$ (**9**) in 40% yield (see below). Reduction of the impure *tert*-butoxide derivative **6** was also examined; although deep purple solutions were obtained that are diagnostic of dinuclear dinitrogen complexes (e.g., both **1** and **9** are dark blue both in solution and in the solid state as is **3**, and **2** is deep brown), crystalline materials could not be isolated and the solution NMR spectra indicated multiple products. Attempts to reduce the diphenylmethoxide complex **7** and the diphenylamide derivative **8** did not lead to any tractable materials, and no evidence of reduction by the formation of colored solutions was obtained. (See Scheme 1.)

The formation of the aryloxide dinitrogen complex **9** was sensitive to the purity of the N_2 atmosphere. Although we routinely passed the N_2 through a MnO/molecular sieve tower to remove trace O_2 and H_2O, the crude reaction mixture obtained from the reduction of **5** under purified tank N_2 possessed a number of impurities as evidenced from $^{31}P\{^1H\}$ NMR spectra. Most of the impurities were hexanes-soluble and could be removed by washing the crude precipitate with hexanes; recrystallization of the remaining material from toluene gave the pure N_2 complex **9** having only a singlet resonance at 8.69 ppm in the $^{31}P\{^1H\}$ NMR spectrum. In contrast, when the reduction was performed under ^{15}N-labeled dinitrogen, $^{15}N_2$, not only were there fewer impurities present but, in addition, two dinitrogen-containing complexes could be isolated, both having the same (but isotopomeric) molecular formula as **9**, in other words, $\{[(Pr^i{}_2PCH_2SiMe_2)_2N]Zr(O\text{-}2,6\text{-}Me_2C_6H_3)\}_2(\mu\text{-}\eta^2\text{:}\eta^2\text{-}{}^{15}N_2)$ (**9**-$^{15}N_2$); presumably, the labeled dinitrogen is of better quality than the unlabeled N_2. The $^{31}P\{^1H\}$ NMR spectrum of the mixture showed three singlets at 8.69, 8.85, and 11.26 ppm in the approximate ratio 4:1:1; assuming that the two new singlets at 8.85 and 11.26 ppm are due to a single isomeric compound, labeled **9a**, then the isomers formed are in a 2:1 ratio with the major isomer, labeled **9**, giving rise to the singlet at 8.69 ppm. The ^{1}H NMR spectral resonances of the mixture are detailed in Table 1. One possible rationalization of the NMR spectral data is that the major isomer **9** has both ends of the dinuclear unit equivalent, while the minor isomer **9a** has inequivalent $Zr(O\text{-}2,6\text{-}C_6H_3)[N(SiMe_2CH_2PPr^i{}_2)_2]$ fragments attached to the bridging N_2 moiety. Since the minor isomer **9a** is more soluble in hexanes, separation of the two isomers can be achieved by washing the solid mixture of **9** and **9a** with hexanes; recrystallization of the remaining material from toluene gives pure **9**. Attempts to obtain pure **9a** have so far failed.

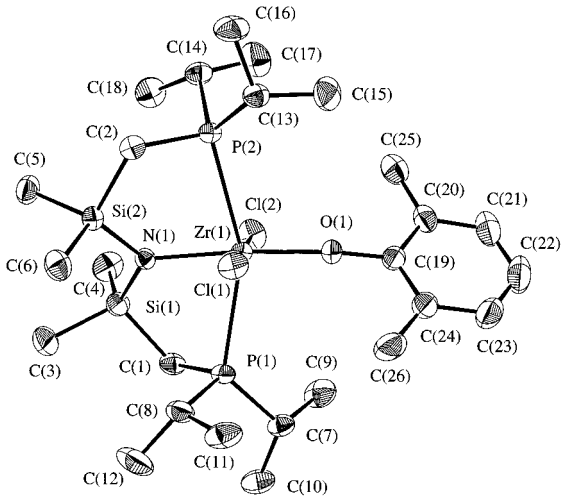

Figure 1. ORTEP drawing showing the molecular structure and numbering scheme for $Zr(O\text{-}2,6\text{-}Me_2C_6H_3)Cl_2[N(SiMe_2CH_2PPr^i{}_2)_2]$ (**5**). Ellipsoids are drawn at the 33% probability level.

Up to this point, we have not presented any data to show that the dinitrogen unit in either **9** or **9a** is side-on bound. As we discussed earlier, differentiating between side-on and end-on coordination of N_2 in a dinuclear complex is difficult. NMR spectral correlations, even ^{15}N NMR chemical shifts, are ambiguous. However, we have shown that resonance Raman spectroscopy has proven diagnostic of the bonding mode and can be correlated to single-crystal X-ray data.[21]

The single-crystal X-ray structure of the major isomer **9** is shown in Figure 2, and selected bond distances and bond angles are given in Table 4. The solid state structure unequivocally shows that the dinitrogen is bound in a side-on fashion bridging the two zirconium centers. The observed nitrogen−nitrogen

(25) Lubben, T. V.; Wolczanski, P. T.; vanDuyne, G. D. *Organometallics* **1984**, *3*, 977.
(26) Cardin, D. J.; Lappert, M. F.; Raston, C. L. *Chemistry of Organo-Zirconium and Hafnium Compounds*, 1st ed.; Ellis Horwood Limited: Toronto, 1986.
(27) Hunter, W. E.; Hrncir, D. C.; Bynum, R. V.; Penttila, R. A.; Atwood, J. L. *Organometallics* **1983**, *2*, 750.

Scheme 1

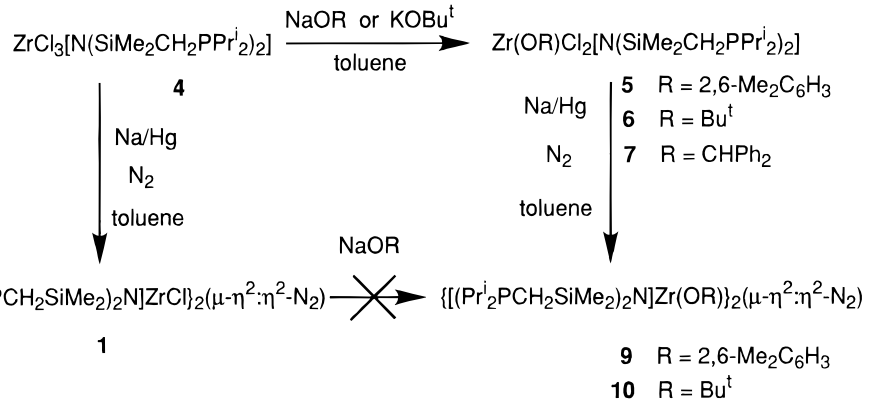

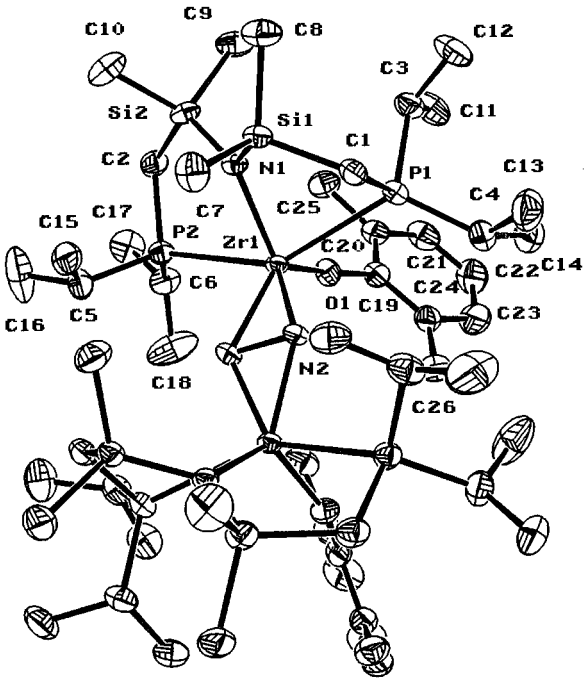

Figure 2. ORTEP drawing showing the molecular structure and numbering scheme for $\{[(Pr^i_2PCH_2SiMe_2)_2N]Zr(O\text{-}2,6\text{-}Me_2C_6H_3)\}_2(\mu\text{-}\eta^2\text{:}\eta^2\text{-}N_2)$ (**9**). Ellipsoids are drawn at the 33% probability level.

bond length of 1.528(7) Å (Table 4) is essentially identical to that (1.548(7) Å) previously reported for the side-on derivative **1** and is significantly longer than the bridging end-on complexes where the nitrogen−nitrogen bond lengths range from 1.12 to 1.3 Å. A compilation of N−N bond lengths (Table 5) provides a comparison with other dinitrogen complexes and also to selected other molecules of interest. The N−N bond lengths in complexes **1** and **9** are not only longer than that of free hydrazine but also longer than that found for the coordinated hydrazine ligand (N_2H_4) or hydrazido ligand $(NHNH)^{2-}$ (Table 5). Another important structural feature is that the bridging N_2 unit is not planar as found for **1** but exhibits a bent or hinged geometry. The hinge angle, defined by the angle between the two ZrN_2 planes, is 156.2°. It can also be seen that the aryloxide substituents lie on the same closed side of the Zr_2N_2 hinge; this is in contrast to that found in **1** where the chloride ligands on Zr are located on opposite sides of the planar Zr_2N_2 core. As will be discussed below, the hinged structural motif can be used to rationalize the observation of structural isomers in the crude reaction mixture of **9**.

The bond distances associated with the phosphine donors and zirconium are comparable to those in other complexes of zirconium that contain this PNP ancillary ligand system. The bond lengths from the zirconium to each of the bridging nitrogens, Zr−N(2), are 2.034(4) and 2.082(4) Å, shorter than the zirconium−amide bond length, Zr−N(1) = 2.211(3) Å, of the ancillary tridentate ligand; similar differences in Zr−N bond distances were observed for the chloride complex **1**. Other zirconium−nitrogen bond distances in the literature range from 1.826(4) Å for a zirconium−nitrogen double bond in $Cp_2Zr=NBu^t(THF)$[28] to 2.443(1) Å in Schiff base chelate derivatives.[29]

The zirconium−oxygen bond separation, Zr−O(1), is 2.020(3) Å and the bond angle defined by the atoms Zr, O(1), and C(19) is 161.5(4)° (Table 4). In the solid state structure of **8**, the aryloxide ligand is oriented such that the methyl substituents are directed away from the isopropyl substituents of the phosphine donors.

The structure of the major isomer **9** having each aryloxide ligand on the same, closed side of the Zr_2N_2 hinge suggests that the minor isomer, **9a**, could have the aryloxide units on opposite sides of the hinged Zr_2N_2 core. Assuming that the Zr_2N_2 core remains hinged, the major isomer **9** has C_{2v} symmetry while the minor isomer has C_s symmetry. Such a proposal is consistent with the NMR spectroscopic parameters of both the major and minor isomers (Table 1); in particular, the dinuclear unit **9a** with C_s symmetry would have inequivalent ends and, as such, would give rise to more complicated ^1H NMR spectral data and should also show inequivalent phosphorus nuclei in the $^{31}P\{^1H\}$ NMR spectrum, exactly in agreement with the data.

To further characterize these complexes, resonance Raman (RR) data were collected for **9**. With excitation at 647.1 nm, two strong bands are observed at 751 and 732 cm^{-1} (Figure 3A). The 751 cm^{-1} peak shifts to 725 cm^{-1}, overlapping with the 732 cm^{-1} band in the spectrum of the $^{15}N_2$ isotopomer and

(28) Walsh, P. J.; Hollander, F. J.; Bergman, R. G. *J. Am. Chem. Soc.* **1988**, *110*, 8729.
(29) Archer, R. D.; Day, R. O.; Illingsworth, M. L. *Inorg. Chem.* **1976**, *18*, 2908.
(30) Wilkinson, P. G.; Hounk, N. B. *J. Chem. Phys.* **1956**, *24*, 528.
(31) Allen, F. H.; Kennard, O.; Watson, D. G.; Brammer, L.; Orpen, A. G.; Taylor, R. *J. Chem. Soc., Perkin Trans. 2* **1987**, S1.
(32) Sutton, L. E. *Tables of Interatomic Distances and Configurations in Molecules and Ions*; Chemical Society: London, 1958; Vol. 11.
(33) Fryzuk, M. D.; Haddad, T. S.; Rettig, S. J. *J. Am. Chem. Soc.* **1990**, *112*, 8185.
(34) Turner, H. W.; Fellmann, J. D.; Rocklage, S. M.; Schrock, R. R.; Churchill, M. R.; Wasserman, H. J. *J. Am. Chem. Soc.* **1980**, *102*, 7810.
(35) Blum, L.; Williams, I. D.; Schrock, R. R. *J. Am. Chem. Soc.* **1984**, *106*, 8316.
(36) Duchateau, R.; Gambarotta, S.; Beydoun, N.; Bensimon, C. *J. Am. Chem. Soc.* **1991**, *113*, 8986.

Table 5. Compilation of Nitrogen−Nitrogen Bond Lengths for Selected Compounds

compound	bond length, Å	ref
N_2	1.0975(2)	30
PhN═NPh	1.255	31
H_2NNH_2	1.46	32
$[(\eta^5\text{-}C_5Me_5)_2Sm[_2(\mu\text{-}\eta^2\text{:}\eta^2\text{-}N_2)$	1.088(12)	15
$\{[(Pr^i_2PCH_2SiMe_2)_2N]ZrCl\}_2(\mu\text{-}\eta^2\text{:}\eta^2\text{-}N_2)$, **1**	1.548(7)	20, 33
$\{[(Pr^i_2PCH_2SiMe_2)_2N]Zr(\eta^5\text{-}C_5H_5)\}_2(\mu\text{-}N_2)$, **2**	1.301(3)	20
$\{[(Pr^i_2PCH_2SiMe_2)_2N]Zr(O\text{-}2,6\text{-}Me_2C_6H_3)\}_2(\mu\text{-}\eta^2\text{:}\eta^2\text{-}N_2)$, **9**	1.528(7)	this work
$[(OEPG)Li(THF)_2]Sm(\mu\text{-}\eta^2\text{:}\eta^2\text{-}N_2)Li_4$	1.525	16
$\{[PhP(CH_2SiMe_2NSiMe_2CH_2)_2PPh]Zr\}_2(\mu\text{-}\eta^2\text{:}\eta^2\text{-}N_2)$, **3**	1.43(1)	19
$\{(Me_3P)_2(Me_3CCH_2)Ta{=}CHCMe_3\}_2(\mu\text{-}N_2)$	1.298(12)	34
$[W(NPh)Me_3]_2(\mu\text{-}\eta^1\text{:}\eta^1\text{-}NH_2NH_2)(\mu\text{-}\eta^2\text{:}\eta^2\text{-}NHNH)$		35
$\mu\text{-}\eta^1\text{:}\eta^1\text{-}NH_2NH_2$	1.434(14)	
$\mu\text{-}\eta^2\text{:}\eta^2\text{-}NHNH$	1.391(15)	
$[\{Li(THF)_3\}_2(\mu\text{-}\eta^2\text{:}\eta^2\text{-}N_2)]^+[\{(\eta^5\text{-}C_5H_5)_2Zr\}_2(\mu\text{-}PPh)_2]^-$	1.06	13
$[\{[(Me_3Si)_2N]_2Ti\}_2(\mu\text{-}\eta^2\text{:}\eta^2\text{-}N_2)_2]^-$	1.379	36

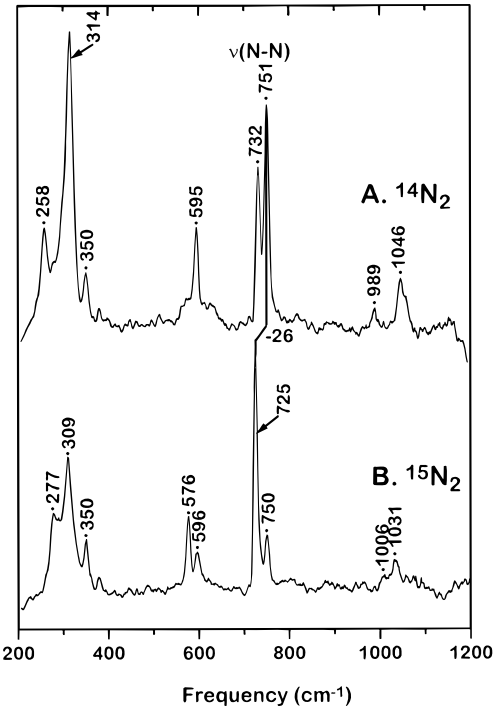

Figure 3. Resonance Raman spectra of **9**: (A) $^{14}N_2$ isotopomer; (B) $^{15}N_2$ isotopomer. Spectra were collected with 647.1 nm excitation (60 mW) at ≈90 K using a scan rate of 1 cm^{-1}/s for nine scans. Each spectrum was 13-point-smoothed and baseline-corrected.

causing its intensity to increase sharply relative to the 751 cm^{-1} band (Figure 3B). This shift from 751 to 725 cm^{-1} is within 1 cm^{-1} of the predicted isotope shift for a pure N−N diatomic oscillator. Consequently, we assign the peak at 751 cm^{-1} to the symmetric ν(N−N) vibrational mode. This frequency is consistent with the long N−N bond distance and the supports the side-on-bonded orientation of the N_2 ligand as found in the crystal structure of **9**. The small residual intensity at 750 cm^{-1} in the $^{15}N_2$ spectrum is probably due to some $^{14}N_2$ contaminant in the $^{15}N_2$ isotopomer. The assignment of the 732 cm^{-1} peak in Figure 3A remains unclear. However, its isotope insensitivity suggests that it may be a ligand mode not associated with the Zr_2N_2 moiety. The weaker bands at 986 and 1046 cm^{-1} may be assigned as combinations between the strong 732 cm^{-1} band and the two isotope-sensitive, low-frequency modes at 258 and 314 cm^{-1}, respectively. Similar combination bands are observed for the $^{15}N_2$ isotopomer at 1006 (732 + 277) and 1031 (732 + 309) cm^{-1}. Similar RR features were observed in the RR spectrum of $\{[(Pr^i_2PCH_2SiMe_2)_2N]ZrCl\}_2(\mu\text{-}\eta^2\text{:}\eta^2\text{-}N_2)$ (**1**), which has a chloride in place of the aryloxide ligand of **9**.[21]

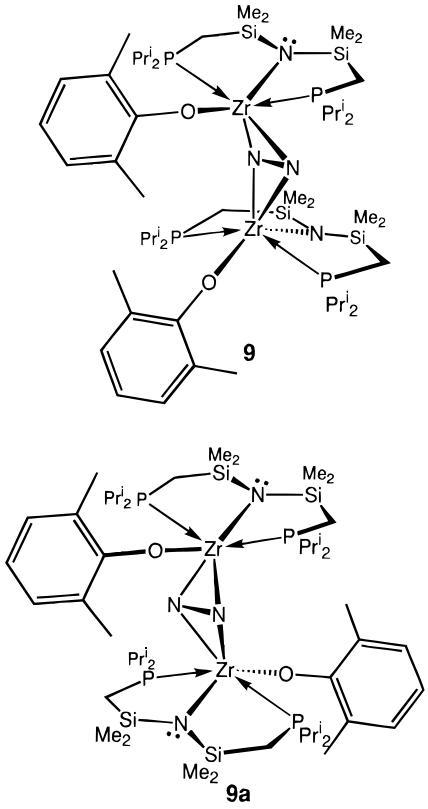

Other peaks in the RR spectrum of **9** also show isotope shifts. To illustrate, there is a peak at 595 cm^{-1} in the spectrum of the $^{14}N_2$ isotopomer (Figure 3A) that forms a doublet in the spectrum of the $^{15}N_2$ isotopomer at 596 and 576 cm^{-1} (Figure 3B). Again, the small peak at 596 cm^{-1} in Figure 3B probably represents some residual $^{14}N_2$ in the $^{15}N_2$ isotopomer. The shift from 595 to 576 cm^{-1} is within 2 cm^{-1} of the shift for a Zr−N stretch predicted by assuming a pure diatomic oscillator. It is interesting to note that no isotope-sensitive stretches assignable to Zr−N modes were observed for **1**, possibly a reflection of the difference in the local symmetry between **1** and **9**. Alternatively, these isotope-sensitive stretches may be due to a Zr_2N_2 cage mode similar to that proposed for the Cu_2O_2 dimer in the $\mu\text{-}\eta^2\text{:}\eta^2\text{-}O_2$ complex of oxyhemocyanin.[37]

Conclusions

In this work we have presented another example of the side-on mode of bonding of a dinitrogen fragment in a dinuclear

(37) Ling, J.; Nestor, L. P.; Czernuszewicz, R. S.; Spiro, T. G.; Fraczkiewicz, R.; Loehr, T. M.; Sanders-Loehr, J. *J. Am. Chem. Soc.* **1994**, *116*, 7682.

metal complex. The use of Zr as the metal center seems to be important, as does the choice of the ancillary ligand. For example, it would appear that replacement of the anionic chloride ligand of **1** by an aryloxide donor does not dramatically affect the frontier orbitals as the side-on mode is observed and, as well, a very long N−N bond length of 1.528(7) Å is found in **9**. However, other attempts to replace the chloride with amide or alkoxide ligands have so far failed to produce isolable N_2 complexes, presumably due to synthetic difficulties.

Acknowledgment. Financial support was generously provided by the NSERC of Canada (M.D.F.) and NIH Grant GM 18865 (T.M.L.).

Supporting Information Available: X-ray crystallographic files, in CIF format, for the structure determinations of **5** and **9** are availasble on the Internet only. Access information is given on any current masthead page.

IC9709786